About the Inclusion of Water in Cu(In,Ga)Se_2 Absorber Material During Accelerated Lifetime Testing

Thierry Kohl,[*,†,‡,¶] N. A. Rivas,[†,‡] J. de Wild,[†,‡,¶] D. G. Buldu,[†,‡,¶] G. Birant,[†,‡,¶] G. Brammertz,[†,‡,¶] M. Meuris,[†,‡,¶] F. Renner,[†,‡] J. Poortmans,[†,¶,§,‖] and B. Vermang[*,†,‡,¶]

†*Institute for Material Research (IMO), Hasselt University (partner in Solliance), Agoralaan gebouw H, Diepenbeek 3590, Belgium.*

‡*imec division IMOMEC (partner in Solliance), Wetenschapspark 1, 3590 Diepenbeek, Belgium.*

¶*EnergyVille, Thorpark, Poort Genk 8310 & 8320, 3600, Belgium.*

§*imec (partner in Solliance), Kapeldreef 75, Leuven, 3001, Belgium.*

‖*Department of Electrical Engineering, KU Leuven, Kasteelpark Arenberg 10, 3001 Heverlee, Belgium.*

E-mail: thierry.kohl@uhasselt.be/thierry.kohl@imec.be; bart.vermang@uhasselt.be

Abstract

To determine if Cu(In,Ga)Se_2 (CIGS) can be submitted to the constraints that will be imposed on the solar materials of the future by an ever growing demand and necessity, we produced ultra-thin (500nm) single-stage coevaporated CIGS solar cells doped with varying amounts and types of alkali atoms. We subjected them to accelerated lifetime testing. In the present work, we observed the seeping of water into the

grain boundaries which could be identified as one of the main culprits for performance degradation. In addition, this phenomenon could only be observed when alkali atoms were present in the absorber layer.

If humanity wants to keep up with the current climate protection goals, we will require a sizeable amount of our daily energy needs to be provided by renewable energy sources like wind, water, and solar power. With regards to solar power, photovoltaic cells need to be increasingly more efficient, and considerably easier and cheaper to produce. Moreover, they need to be suited to endure long lasting operation times. Thin-film solar cells, such as $Cu(In,Ga)Se_2$ (CIGS), are one of the most viable candidates for these solar cells of the future as they have already achieved high efficiencies upwards of 23%[1]. Additionally, these thin-film cells are the most suited for building-integrated photovoltaics which in itself constitutes one of the most promising routes into a greener future.

In order to achieve the highest efficiencies of CIGS thin film solar cells, alkali doping has become a necessary step[2–4]. However, it was previously shown, that a higher concentration of alkali atoms will lead to more pronounced declines in the cells efficiency over its lifetime[5–7]. Companies need to be able to guarantee that solar cells will produce 80% or more of their original performance over a timespan ranging from 20 to 25 years. In this sense, thorough reliability studies of a solar cell, as well as the mechanisms that provoke its eventual failure is, thus, of the utmost importance.

Various past reliability experiments, performed on the separate parts of the solar cells, have already taught us a lot about how different elements of a functional solar cell degrade over their lifetime[5–10]. Nevertheless, the exact degradation and failure mechanisms of alkali doped CIGS solar cells, are still widely unknown and require further investigation. A proper control of the alkali atoms during the growth and ageing of CIGS has become increasingly important as modern CIGS is more regularly deposited on substrates such as polyimide or stainless-steel[11]. On top of being flexible, these substrates have the particularity of not providing any alkali atoms during processing, as opposed to the CIGS substrates like glass.

The absorber material is deposited by using a one-stage coevaporation process. This deposition process is simple and produces a flat and homogeneous Ga profile[12]. In order to make the production process of CIGS more cost-effective, we opted to deposit the absorber material in ultra-thin (400-500nm) layers. By reducing the amount of bulk material, the aim is to limit the use of scarcer elements like In and Ga as much as possible. Another particularity of this deposition approach is that it ensures that we deposit CIGS material with a very low average grain size (<100nm), as can be seen in figure 1, which is an advantage is one wants the study the material's grain boundaries.

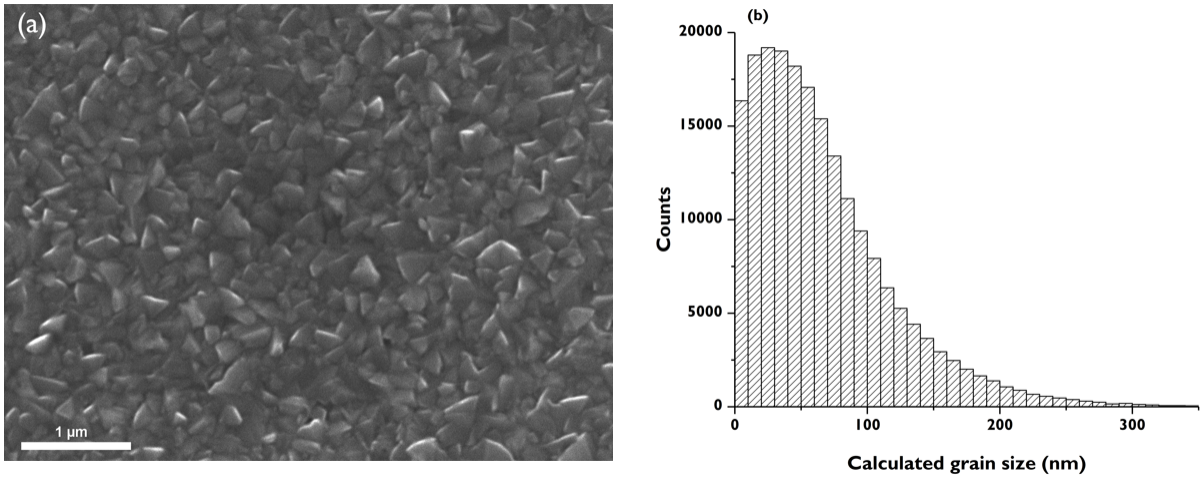

Figure 1: Example of a typical 1-stage CIGS surface as observed with SEM (a). Calculated typical grain size distribution for a standard 1-stage CIGS absorber, as extracted by the program Gwyddion (b).

In the present case, the CIGS layers are deposited on soda-lime glass (SLG) equipped with a Si(O,N) diffusion barrier and a Molybdenum back contact. The barrier prevents the diffusion of alkali atoms from the SLG into the CIGS and allows for a better control of the concentration of alkali atoms in the layer. Additionally, it allows for a better isolation of the effects of the different elements by preventing an uncontrolled mix of alkali from being present in the absorber material. Thereby, it helps to simulate the cases in which alkali-free substrates are used as a base for the growth of the CIGS absorber. All alkalis are deposited in their fluoride form (NaF, KF, etc.) either by evaporation, prior to CIGS deposition, or

by a post-deposition treatment, through spin-coating followed by heat treatment[12]. After deposition of the absorber material, we followed the generally accepted standard for CIGS solar cells, by depositing a thin (∼50nm) CdS buffer layer by chemical bath deposition and a i-ZnO/Al:ZnO window layer (TCO) by sputtering. Once finished, we submitted the unencapsulated cells to accelerated lifetime testing (ALT) under highly degrading conditions in an 85°C/85% room humidity damp heat environment. This aggressive setting is expected to simulate standard outdoor condition equivalent to 20 years in an experimentally reasonable timespan of a 1000 hours. As they age, the solar cells performance is monitored by regular IV measurements. These IV measurements showed similar behavior for all the studied samples, independent of their composition. In all cases, both short-circuit current and open-circuit voltage stayed constant all through the experiment. However, the efficiency of the cells drops by an average 40% over the course of the experiment. This degradation is due to a progressive change in fill-factor. This change can be explained by a combined increase in series resistance (Rs) and decrease in shunt resistance (Rsh). The increase in the Rs was expected given what was previously known about the degradation of the TCO. Indeed, under the influence of water, the standard window layer for CIGS tends to progressively loose its conducting properties[9]. Any changes in the Rsh, however, are in general much more difficult to explain[13]. Nevertheless, we noticed that, in the present case, the decrease Rsh was significantly slower for the sample without added alkali atoms, which motivated our further investigation. The terminally degraded cells as well as some reference samples are then further analyzed using atom probe tomography (APT) to study them on an atomic level and determine what happened to the material itself during degradation. To do so, they were prepared into bullet-shaped specimens using a focused-ion-beam (FIB). These specimens have a tip width below 100nm and a base width of up to 1μm with a height below 2 μm.

Given that the average size of the grains in our material is very low, the probability that the APT specimen contained at least one grain boundary after FIB preparation is substantial. We could, thus, very clearly investigate the chemical distribution within grains

but also at the grain boundaries between them and, by doing so, get a very detailed look at the material composition and the state of the absorber materials both before and after degradation.

As a first experiment, two sets of specimens were prepared. Both sets were from the same sample, namely, treated with KF and our standard 2nm NaF predeposition. The first set was used as a reference while the samples in the second set were exposed to the ageing treatment. By performing APT measurements on these specimens, we were then able to compare the chemical composition of the samples before and after ageing.

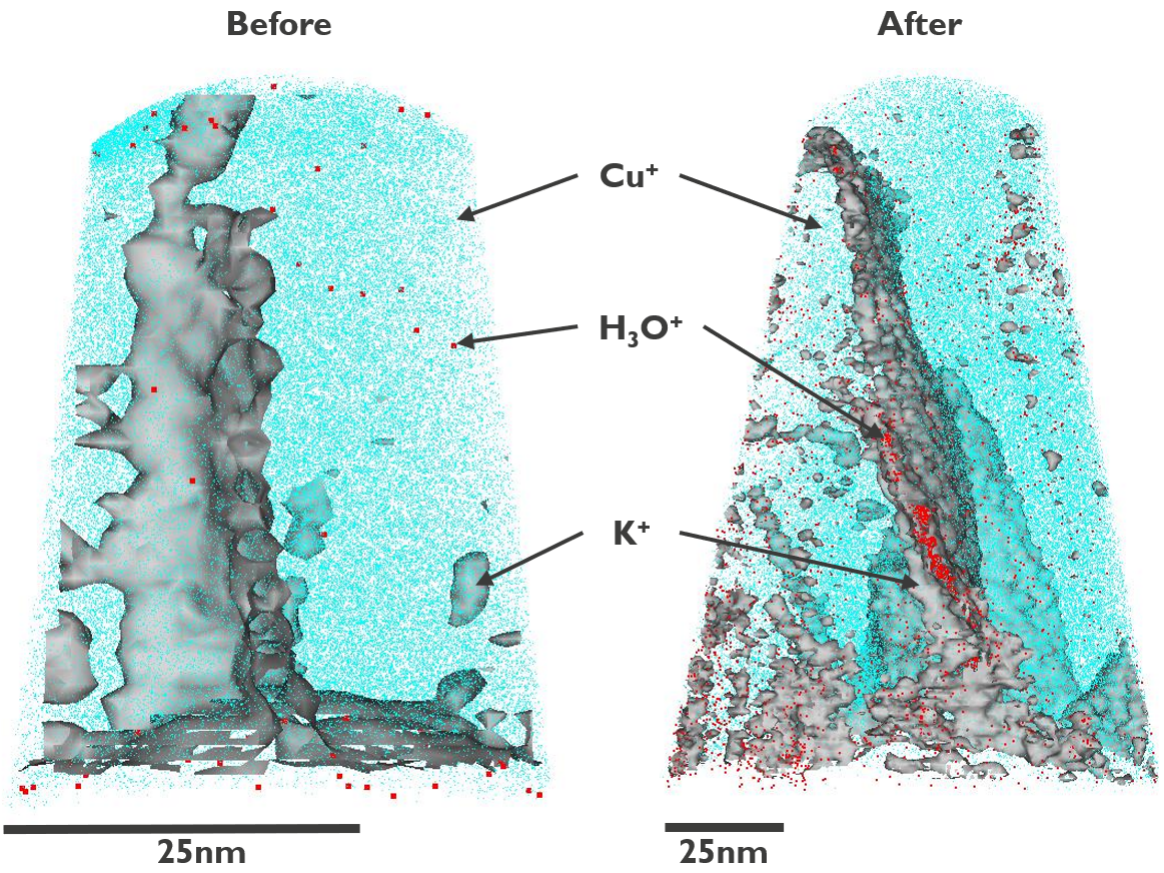

Figure 2: Comparison of the APT specimens of the reference (before) and aged (after) part of the Potassium treated sample. Cu ions are represented in blue, and water ions in red. Potassium is represented in the form of a grey isosurface. Na is not represented on the present figure to avoid overcrowding the pictures, but is mostly located at the bottom of the specimen. The isosurface allows for an easy visualization of the grain boundary. It is clearly visible, when comparing both pictures that the aged specimen has a very high concentration of water ions in the grain boundary, whereas the reference showcases an almost complete absence of water. The water ions that are visible in the reference specimen had to be enhanced 5-fold to be visible.

It appeared that in both cases, the grain boundaries showcase a very high presence of K. This is in good agreement with the most popular theories surrounding the behavior of alkalis[14–23]. In addition to the presence of K, it was possible to detect a consequent amount of H_3O^+ ions in the grain boundary of the aged sample. No significant amount of water ions could be detected in the reference tip, meaning that this must be a consequence of the ageing of the sample. In addition, the concentration of water ions is significantly lower in the grains, showing that the grain boundaries act as the main storage and transport locations

for the water.

We could answer the question about the true origin of the water signal by analyzing the mass spectra of our specimen in detail. Indeed, oxygen has been routinely observed in the past[20,21,23], meaning that the observation of water related mass peaks could be a coincidental ion combination during the recording. However, given the extreme conditions the samples were submitted to during the damp heat treatment, it is more than likely that they show a very high presence of water. Nevertheless, other ions and ion combinations, like F^-, have identical mass to charge ratios to ions like H_3O^+. The former was discarded for two main reasons. First, F^- is a negative ion, meaning it can not be observed using the same potential as positive ions which were probed in the present case. Then, if F^- was the ion responsible for the peak at a mass/charge ratio of 19, it would have been present in the reference specimens as well, since the alkali atoms are deposited in their fluoride form. This was not the case as can be seen in figure 2. In addition to this, alongside the peak at 19, we observed an accompanying peak at a mass/charge ratio of 18. This peak could be a response of H_2O^+ ions. Both ions are positive, which means that they can indeed be observed using the same potential settings.

To verify if the grain boundaries of our material always contain water when aged, we prepared a third and fourth set of tips from two different aged samples. The third set being from the sample with a high amount of predeposited NaF (10nm) and the fourth set being without a specific alkali treatment. The third set revealed similar trends to the first one, showing a very high presence of water in the grain boundary.

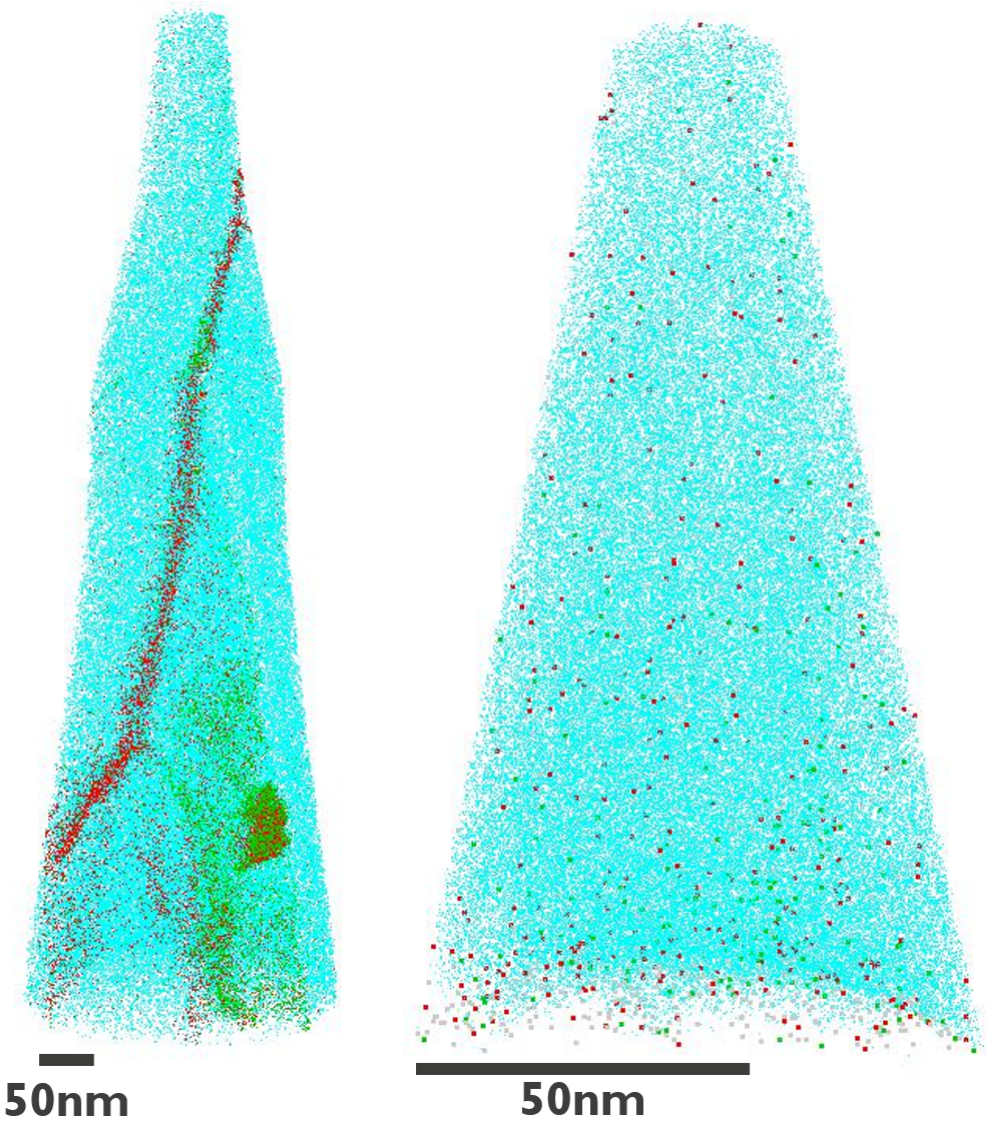

Figure 3: Reconstruction of the APT specimens of the aged samples with sodium (left) and without alkali (right). Cu ions are represented in blue, water ions in red. Na is represented in green. For the sodium containing samples, once again, water is present throughout the entire APT specimen but also clearly segregated in the grain boundary and other defects. The water and sodium ions in the specimen without alkali were enhanced 5-fold to be visible.

The fourth set, in turn, did not show significant presence of water after degradation. As expected, the sample also seems to be mostly clear of alkali atoms. All alkali ions that were detected are mostly randomly distributed all over the specimen and more often localized at its extremities. This is most likely due to the FIB preparation, since it can cause contamination of the outside surfaces of the specimen.

Since site-specific FIB preparation of the CIGS material[24] was not carried out in this study, multiple APT specimens were measured on the sample without alkali. This was done in order to exclude the possibility of the absence of grain boundaries within the final specimens. In this case, all APT measurements indicated the same result, namely, an almost complete absence of water in the measured APT specimen, independent of their size. Since the SEM measurements revealed that all absorber layers have an average grain size below 100 nm, it makes it highly unlikely that the whole set of measured APT specimens would have failed to include a grain boundary. Because of this observation, we concluded that even though water seeps into the grain boundaries of the material, this phenomenon does not take place in the absence of alkali atoms in the sample.

Table 1: Table of the concentration of relevant atoms extracted from the measured APT specimens

Investigated Ion	Potassium Treated Sample	Sodium Treated Sample	Alkali-free Sample
Na	3.56×10^{-4} $at.\%$	3.12×10^{-4} $at.\%$	2.20×10^{-5} $at.\%$
K	4.81×10^{-3} $at.\%$	4.72×10^{-5} $at.\%$	2.48×10^{-4} $at.\%$
H_3O^+	1.53×10^{-3} $at.\%$	1.55×10^{-3} $at.\%$	6.70×10^{-6} $at.\%$

An additional proof for the absence of water in the alkali-free sample can be found in table 1. Indeed, with an average water concentration of 6.70×10^{-6} in the measured specimens, their humidity accumulation is 3 orders of magnitude below what was observed for the alkali containing samples.

As a last test, and since it was expected that due to the small grains in our absorber material our specimen should contain grain boundary, we tried to identify them by analyzing more in detail the Cu content of the measurements. Indeed, it was observed before that grain boundaries typically showcases slight changes in CIGS composition. Most notably, it is possible to observe a characteristic changes in Cu content[20,21,23]. By creating an isosurface with a lower Cu concentration (21%) we were able to localize areas of our specimens that would most likely be a boundary region.

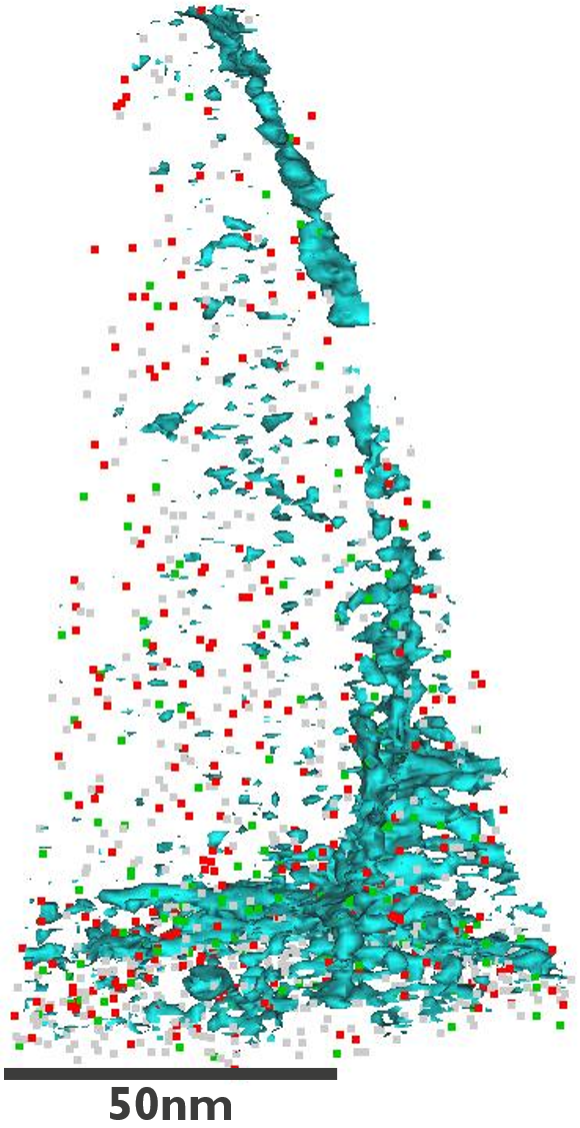

Figure 4: Reconstruction of the APT specimen without alkali treatment. The blue Cu ions are replaced by a Cu 21 % concentration isosurface. This is most likely a grain boundary. This region of the specimen does not show a significant difference in concentration of Alkali and water ions, which were enhanced 5-fold to be visible.

The distribution of water ions detected in this measurement is reasonably random. In addition, their overall concentration is orders of magnitude lower than in the other samples. We, therefore, conclude beyond reasonable doubt that water ingress did not happen in the absence of alkali atoms.

This result is significant, because the seeping of water is one possible explanation for the decreases in shunt resistance that were observed during the electrical characterization

of these samples. Indeed, even though the performance of all samples degraded eventually, the sample without alkali treatment showcased a high resilience to shunting until the very late stages of the degradation, upwards of 750h of damp-heat treatment. To the contrary, the samples with alkali already show significant degradation of Rsh at much earlier stages of the experiment, as early as 250h. All of this means that the presence of alkali can be linked directly to the seeping of water, which, in turn, can be related to observed increases in shunting. Since in the absence of alkali, the Rsh still eventually deteriorates, the presence of water in the grain boundaries can, however, not be identified as the only reason for the degradation of the shunt resistance.

To summarize, our APT results have shown that water is seeping into the absorber layer as the sample ages. In addition, we also measured a significantly lower concentration of water in the samples that had no particular alkali treatment applied to them. This indicates that the seeping of water into the solar cells is exacerbated by the presence of alkali elements in the absorber layer. Thus, a special focus should be given to protecting the solar cells from humidity since a large variety of alkali atoms are routinely added into the preparation of the modern CIGS absorber layers. Moreover, the presence of the water in the grain boundaries is also one possible explanation of the decrease in shunt resistance observed during IV measurements. Indeed, water could promote the conduction of charge carriers through the grain boundaries and, thus, lead to the increased shunting. With this information, one could easily imagine that it might be possible to reverse the ageing of CIGS solar cell affected by water. Indeed, it might be possible to remove the water from its locations in the grain boundaries, given a suitable heat treatment. A replacement of the TCO to counteract the increase in series resistance could then possibly lead to a solar cell with a fully or partially restored conversion efficiency. Further research is currently being focused towards testing this hypothesis.

Acknowledgement

This work received funding from the European Unions H2020 research and innovation program under grant agreement No. 715027.

References

(1) Hutchins, M. Solar Frontier hits n ew CIS cell efficiency record. 2019; https://www.pv-magazine.com/2019/01/21/solar-frontier-hits-new-cis-cell-efficiency-record/.

(2) Salome, P. M.; Hultqvist, A.; Fjallstrom, V.; Edoff, M.; Aitken, B. G.; Zhang, K.; Fuller, K.; Kosik Williams, C. Incorporation of Na in Cu(In,Ga)Se2 thin-film solar cells: A statistical comparison between Na from soda-lime glass and from a precursor layer of NaF. *IEEE Journal of Photovoltaics* **2014**, *4*, 1659–1664.

(3) Chiril, A.; Reinhard, P.; Pianezzi, F.; Bloesch, P.; Uhl, A. R.; Fella, C.; Kranz, L.; Keller, D.; Gretener, C.; Hagendorfer, H.; Jaeger, D.; Erni, R.; Nishiwaki, S.; Buecheler, S.; Tiwari, A. N. Potassium-induced surface modification of Cu(In,Ga)Se2 thin films for high-efficiency solar cells. *Nature Materials* **2013**, *12*, 1107–1111.

(4) Jackson, P.; Wuerz, R.; Hariskos, D.; Lotter, E.; Witte, W.; Powalla, M. Effects of heavy alkali elements in Cu(In,Ga)Se2 solar cells with efficiencies up to 22.6%. *Physica Status Solidi - Rapid Research Letters* **2016**, *10*, 583–586.

(5) Theelen, M.; Barreau, N.; Daume, F.; Steijvers, H.; Hans, V.; Liakopoulou, A.; Vroon, Z.; Zeman, M. Accelerated performance degradation of CIGS solar cell determined by in-situ monitoring. *Reliability of Photovoltaic Cells, Modules, Components, and Systems VII* **2014**, *9179*, 91790I.

(6) Theelen, M.; Barreau, N.; Hans, V.; Steijvers, H.; Vroon, Z.; Zeman, M. Degradation of

CIGS solar cells due to the migration of alkali-elements. *2015 IEEE 42nd Photovoltaic Specialist Conference, PVSC 2015* **2015**,

(7) Theelen, M.; Steijvers, H.; Bakker, K.; Vink, J.; Mortazavi, S.; Mulder, A.; Barreau, N.; Roosen, D.; Haverkamp, E. The exposure of CIGS solar cells to different electrical biases in a damp-heat illumination environment. *2017 IEEE 44th Photovoltaic Specialist Conference, PVSC 2017* **2017**, 1–6.

(8) Theelen, M.; De Amorim Soares, G.; Beyeler, K.; Steijvers, H.; Barreau, N. Stability of unpackaged CIGS solar cells under illumination with damp heat, dry heat and dry cold followed by cycling. **2017**, *1037009*, 7.

(9) Theelen, M. Degradation of Cigs Solar Cells. Ph.D. thesis, Technische Univerteit Delft, 2015.

(10) Daume, F.; Puttnins, S.; Scheit, C.; Zachmann, H.; Rahm, A.; Braun, A.; Grundmann, M. Damp heat treatment of Cu(In,Ga)Se2 solar cells with different sodium content. *Materials* **2013**, *6*, 5478–5489.

(11) Kessler, F. Flexible Solar Cells and Modules. `https://www.zsw-bw.de/en/research/photovoltaics/topics/flexible-solar-cells-and-modules.html`.

(12) de Wild, J.; Buldu, D. G.; Schnabel, T.; Simor, M.; Kohl, T.; Birant, G.; Brammertz, G.; Meuris, M.; Poortmans, J.; Vermang, B. High Voc upon KF Post-Deposition Treatment for Ultrathin Single-Stage Coevaporated Cu(In, Ga)Se2 Solar Cells. *ACS Applied Energy Materials* **2019**, *2*, 6102–6111.

(13) Williams, B. L.; Smit, S.; Kniknie, B. J.; Bakker, K. J.; Keuning, W.; Kessels, W. M. M.; Schropp, R. E. I.; Creatore, M. Identifying parasitic current pathways in CIGS solar cells by modelling dark J V response Identifying parasitic current pathways in CIGS solar. **2015**,

(14) Vilalta-Clemente, A.; Raghuwanshi, M.; Duguay, S.; Castro, C.; Cadel, E.; Pareige, P.; Jackson, P.; Wuerz, R.; Hariskos, D.; Witte, W. Rubidium distribution at atomic scale in high efficient Cu(In,Ga)Se2 thin-film solar cells. *Applied Physics Letters* **2018**, *112*.

(15) Crossbeam, Z.; ORION NanoFab, Z.; ORION NanoFab Authors, Z.; Pérez-Willard, F.; Khanom, F.; Huynh, C.; Notte, J.; Magorian Friedlmeier, T. Alkali Diffusion in CIGS Solar Cells Studied by Gallium and Neon SIMS. *Zeiss White Paper* **2019**,

(16) Schöppe, P.; Schönherr, S.; Jackson, P.; Wuerz, R.; Wisniewski, W.; Ritzer, M.; Zapf, M.; Johannes, A.; Schnohr, C. S.; Ronning, C. Overall Distribution of Rubidium in Highly Efficient Cu(In,Ga)Se2 Solar Cells. *ACS Applied Materials and Interfaces* **2018**, *10*, 40592–40598.

(17) Pianezzi, F.; Reinhard, P.; Chiril, A.; Bissig, B.; Nishiwaki, S.; Buecheler, S.; Tiwari, A. N. Unveiling the effects of post-deposition treatment with different alkaline elements on the electronic properties of CIGS thin film solar cells. *Physical Chemistry Chemical Physics* **2014**, *16*, 8843–8851.

(18) Nicoara, N.; Manaligod, R.; Jackson, P.; Hariskos, D.; Witte, W.; Sozzi, G.; Menozzi, R.; Sadewasser, S. Direct evidence for grain boundary passivation in Cu(In,Ga)Se2 solar cells through alkali-fluoride post-deposition treatments. *Nature Communications* **2019**, *10*, 1–8.

(19) Muzzillo, C. P.; Poplawsky, J. D.; Tong, H. M.; Guo, W.; Anderson, T. Revealing the beneficial role of K in grain interiors, grain boundaries, and at the buffer interface for highly efficient CuInSe2 solar cells. *Progress in Photovoltaics: Research and Applications* **2018**, *26*, 825–834.

(20) Raghuwanshi, M.; Cadel, E.; Duguay, S.; Arzel, L.; Barreau, N.; Pareige, P. Influence of Na on grain boundary and properties of Cu(In,Ga)Se2 solar cells. *Progress in Photovoltaics: Research and Applications* **2017**, *25*, 367–375.

(21) Raghuwanshi, M.; Vilalta-Clemente, A.; Castro, C.; Duguay, S.; Cadel, E.; Jackson, P.; Hariskos, D.; Witte, W.; Pareige, P. Influence of RbF post deposition treatment on heterojunction and grain boundaries in high efficient (21.1%) Cu(In,Ga)Se 2 solar cells. *Nano Energy* **2019**, *60*, 103–110.

(22) Stokes, A.; Al-Jassim, M.; DIercks, D.; Clarke, A.; Gorman, B. Impact of Wide-Ranging Nanoscale Chemistry on Band Structure at Cu(In, Ga)Se2 Grain Boundaries. *Scientific Reports* **2017**, *7*, 1–11.

(23) Cojocaru-Mirédin, O.; Choi, P. P.; Abou-Ras, D.; Schmidt, S. S.; Caballero, R.; Raabe, D. Characterization of grain boundaries in Cu(In,Ga)Se 2 films using atom-probe tomography. *IEEE Journal of Photovoltaics* **2011**, *1*, 207–212.

(24) Schwarz, T.; Stechmann, G.; Gault, B.; Cojocaru-Mirédin, O.; Wuerz, R.; Raabe, D. Correlative transmission Kikuchi diffraction and atom probe tomography study of Cu(In,Ga)Se2 grain boundaries. *Progress in Photovoltaics: Research and Applications* **2018**, *26*, 196–204.